

Western University

Scholarship@Western

Electrical and Computer Engineering
Publications

Electrical and Computer Engineering
Department

2019

A virtual-reality training simulator for cochlear implant surgery

Blake Jones

The University of Western Ontario, bjones82@uwo.ca

Seyed Alireza Rohani

The University of Western Ontario, srohani4@uwo.ca

Nelson Ong

The University of Western Ontario, nong2@uwo.ca

Tarek Tayeh

The University of Western Ontario, ttayeh@uwo.ca

Hanif M. Ladak

The University of Western Ontario, hladak@uwo.ca

See next page for additional authors

Follow this and additional works at: <https://ir.lib.uwo.ca/electricalpub>



Part of the [Biomedical Engineering and Bioengineering Commons](#), and the [Electrical and Computer Engineering Commons](#)

Citation of this paper:

Jones, Blake; Rohani, Seyed Alireza; Ong, Nelson; Tayeh, Tarek; Ladak, Hanif M.; Chalabi, Ahmad; and Agrawal, Sumit K., "A virtual-reality training simulator for cochlear implant surgery" (2019). *Electrical and Computer Engineering Publications*. 591.

<https://ir.lib.uwo.ca/electricalpub/591>

Authors

Blake Jones, Seyed Alireza Rohani, Nelson Ong, Tarek Tayeh, Hanif M. Ladak, Ahmad Chalabi, and Sumit K. Agrawal

1 **A virtual-reality training simulator for cochlear implant surgery**

2 Blake Jones, Seyed Alireza Rohani, Nelson Ong, Tarek Tayeh, Ahmad Chalabi, Sumit K

3 Agrawal*, Hanif M Ladak*

4 *co-senior authors

5

6 **Abstract**

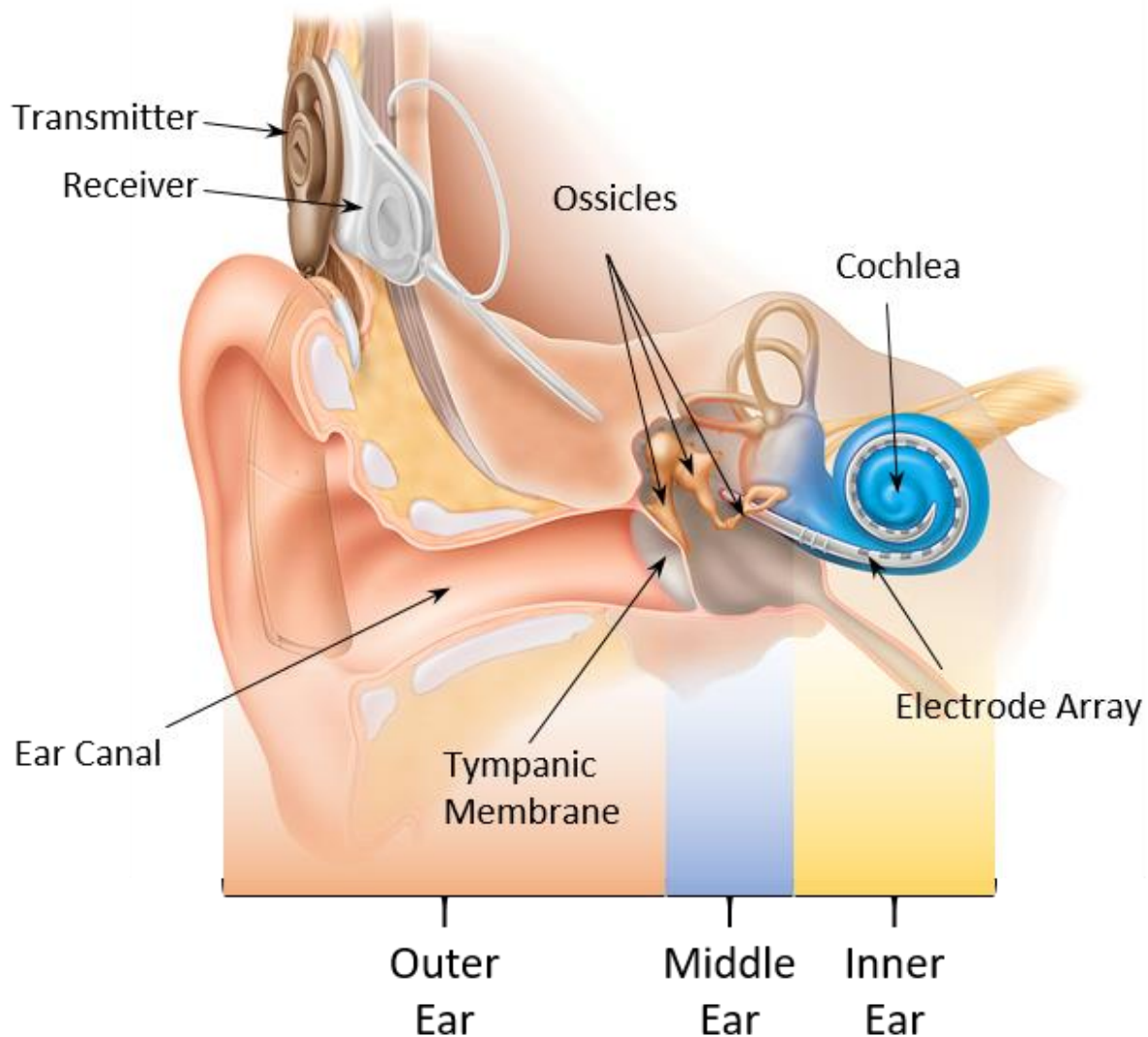
7 **Background and Objectives:** Hearing loss is one of the most prevalent chronic conditions and
8 can significantly impact an individual's quality of life. Cochlear implantation (CI) is a widely
9 applicable treatment for severe to profound hearing loss, however CI surgery can be difficult for
10 surgical trainees to master. Training environments that are safe, controlled, and affordable are
11 needed. To this end, we present a virtual-reality (VR) cochlear implant surgical simulator
12 developed with a popular, commercial game engine. **Method:** Unity3D was used to develop the
13 simulator and model the delicate instruments involved. High-resolution models of human
14 cochleae were created from images obtained from synchrotron-radiation phase-contrast imaging
15 (SR-PCI). The physical-realism of the simulator was assessed via a comparison with
16 fluoroscopic images of an actual cochlear implant insertion. Different resolutions of cochlear
17 models were used to benchmark the real-time capabilities of the simulator with the number of
18 frames per second (FPS) serving as the performance metric. **Results:** Quantitative analysis
19 comparing the simulated procedure to fluoroscopic imaging revealed no significant differences.
20 Qualitatively, the behaviour of the inserted and simulated implants were similar throughout the
21 entirety of the procedure. The simulator was able to maintain 25 FPS even when experiencing an

22 artificially high computational load. **Conclusion:** VR simulators provide a new and exciting
23 avenue to enhance current medical education. Continued use of widely available and supported
24 game engines in the development of medical simulators will hopefully result in lowered costs.
25 Preliminary feedback from expert surgeons of the simulator presented here has been positive and
26 future work will focus on evaluating face, content and construct validity.

27 **Keywords:** simulation, surgical training, cochlear implants, gaming engines

28 **1. Introduction**

29 One of the fundamental ways that humans interact with the world is through sound. Speech, tone
30 and other verbal cues play a vital role in human communication. For these reasons, hearing loss
31 can have devastating implications on an individual's quality of life. The anatomy that facilitates
32 hearing is diverse in both function and form, as are the causes of hearing loss. Damage to any
33 one of the tympanic membrane (eardrum), the ossicles (delicate bones of the middle ear), or the
34 cochlea (spiral-shaped bone that transmits sound to the nervous system) may result in partial or
35 complete loss of hearing.



36

37 **Figure 1.** Ear anatomy and cochlear implant components. (Wikimedia Commons, 2008)

38 Cochlear implantation (CI) is a surgical procedure that aims to remedy severe to profound
 39 sensorineural hearing loss via the insertion of a thin, conducting electrode into the cochlea.

40 Figure 1 presents a simplified view of a cochlear implant and relevant ear anatomy. The

41 transmitter of the CI contains the microphone and processor. This sends the processed sound

42 signals and energy to the implanted receiver via radio frequency transmission. The electrode

43 permanently resides within the cochlea, where it directly stimulates the auditory nerve. Cochlear

44 implantation differs from hearing aids in that it does not amplify sound from the environment,

45 but instead directly translates sound into an electrical signal. Since the advent of the modern
46 cochlear implant in 1977, over 300,000 devices have been implanted in patients around the world
47 (NIDCD, 2017). With reports predicting that the cochlear implant market will continue its
48 growth and reach 3.1 billion USD by 2025 (Grand View Research, 2017) the need for trained
49 surgeons to perform these implants is increasing.

50 The cochlear implantation procedure consists of three parts: 1) incision and drilling of the
51 mastoid process (bone located immediately behind the ear), 2) implantation of the internal
52 receiver into the mastoid process, and 3) insertion of the electrode into the cochlea. Electrode
53 insertion is especially important, since the final positioning of the electrode may have profound
54 implications on patient-related outcomes (Finley *et al*, 2009). In addition, the insertion process is
55 associated with risk to the fragile anatomical features of the cochlea which, if damaged, can
56 worsen the hearing of a patient (Connell, Hunter, & Wanna, 2016). Surgeons must use
57 meticulous surgical technique and tactile feedback to ensure atraumatic insertions.

58 The traditional method of surgical education is an apprenticeship approach that is rooted in
59 William Stewart Halsted's motto of "See one, do one, teach one." Although refined over the
60 years, the core of this pedagogical formalism has remained a cornerstone of surgical education.
61 However, recent studies assessing the learning curve in new surgical techniques, particularly
62 laparoscopic procedures, have found that the number of surgeries required for surgeons to perfect
63 their abilities can range from 250-750 (Coles, Meglan, & John, 2011; Secin *et al.*, 2012). It is
64 therefore not surprising that Halsted's approach has been the topic of much criticism, and calls
65 for new tools in medical education have been made (Kotsis & Chung, 2013).

66 One such tool that has become increasingly popular is computer-based surgical simulation. With
67 the recent advancements in technology, computer simulation has become an effective option to
68 help train surgical residents (Nagendran, Gurusamy, Aggarwal, Loizidou, & Davidson, 2013). In
69 addition to providing a novel tool with which to train, the digital nature of these systems lends
70 itself well to providing detailed, quantitative feedback, which can facilitate user learning.

71 A critical shortcoming of many early surgical simulators was the inability to provide a tactile
72 response. The importance of a realistic sense of touch in surgical skill development has been
73 noted in the literature, and incorporation of haptic devices into surgical simulators has become
74 essential (Escobar-Castillejos, Noguez, Neri, Magana, & Benes, 2016; Prasad, Manivannan,
75 Manoharan, & Chandramohan, 2016).

76 Although simulators show promise in facilitating higher throughput of well-trained clinicians,
77 the technical burden of developing a new simulator can be high particularly as a result of the
78 low-level languages many modelling frameworks are written in. To this end, this work presents a
79 virtual-reality (VR) simulator for cochlear electrode insertion that incorporates haptic feedback
80 to provide an immersive, realistic experience, which may augment surgical skill development
81 during the preclinical stage of medical education which was developed entirely using a popular,
82 commercial game engine.

83 **2. Methods**

84 **2.1 System Usage**

85 High resolution models of the cochlea are imported into Unity3D (Unity Technologies, San
86 Francisco CA). To begin, the user may select from one of these preloaded options or import their
87 own model. After selection, the chosen model and the electrode are rendered into the scene.

88 The haptic device is now the primary user interface with the system and has control over the
89 position and rotation of the cochlea and electrode, which move synchronously with one another.
90 By translating and rotating the haptic arm, the user can align the scene to their preferred
91 orientation. The outward walls of the models can also be made transparent for increased
92 visualization of the interior structures.

93 Upon positioning the scene to his/her satisfaction, the user can press a button on the haptic arm
94 which detaches the cochlea model from the haptic device. The electrode now moves
95 independently of the cochlea and electrode insertion can begin. Throughout the insertion, usage
96 statistics and performance metrics are tracked to provide feedback. Performance metrics include:
97 insertion time, number of successful insertions, failed attempts, average insertion depth, total
98 time spent training, and number of simulator resets. The user continues inserting the electrode
99 until they indicate they are done or would like to restart. After training is complete, the user may
100 review the performance data that was collected and debrief on their experience.

101

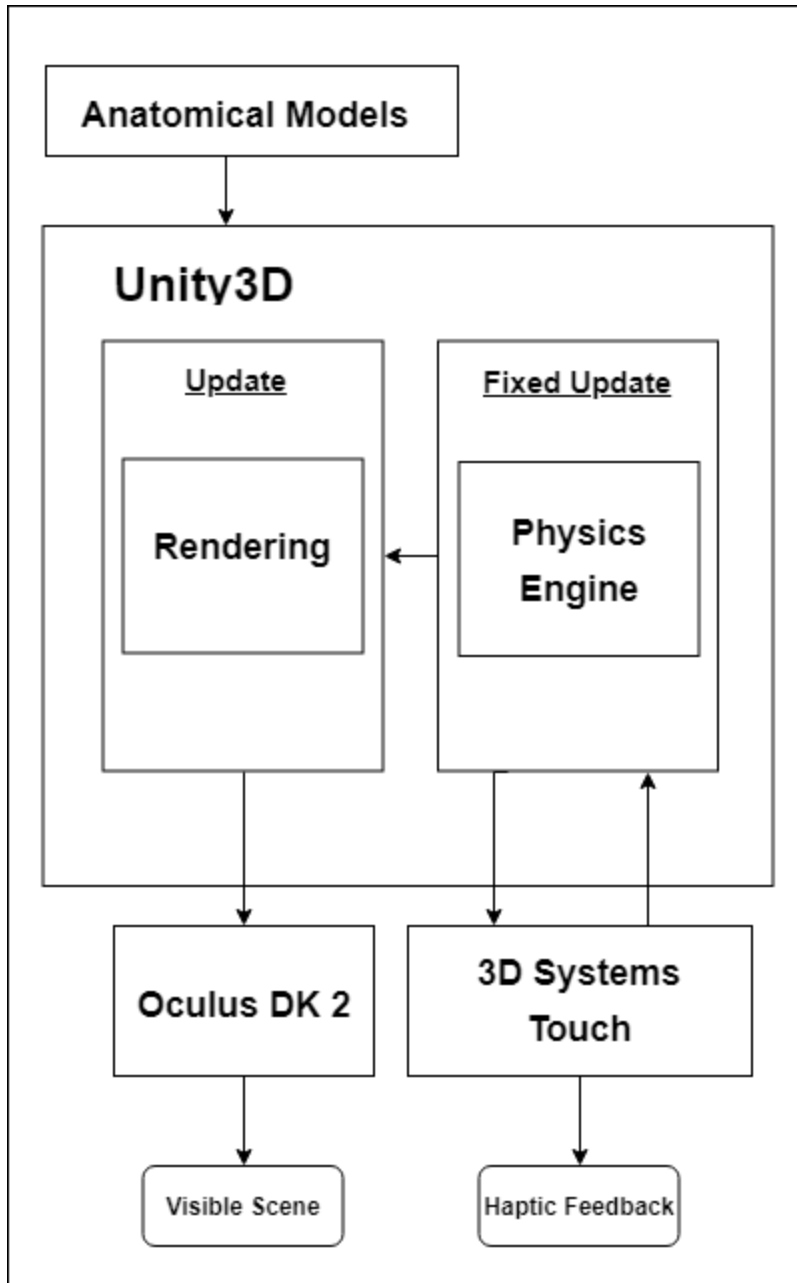
102 **2.2 System Design**

103 The simulator was created using the popular game development platform Unity3D (Unity
104 Technologies, San Francisco, CA). Unity3D is fully compatible with the Windows graphic APIs
105 Direct3D and Direct X 12, and fully supports NVIDIA VRWorks. Unity3D served as a hub to
106 integrate the various components, handle the graphic and haptic rendering, and perform the
107 physical modelling. A diagram of the system architecture is shown in Figure 2.

108 Although Unity3D provides a GUI to streamline the development process, additional C# code
109 was required to implement the flexible electrode, customize the VR experience, interface with

110 the haptic device, and provide debriefing data. Unity3D relies on the Update and FixedUpdate
111 functions to handle visual updates and physical calculations, respectively. Therefore, efforts were
112 made to keep these functions as simple as possible and make use of event-driven programming
113 to increase efficiency.

114 When the simulation begins, the Unity3D game-loop starts. This consists of repeated calls to
115 Update and FixedUpdate. FixedUpdate calculates the position of all the meshes included in the
116 scene and communicates with the haptic C# wrappers which, in turn, communicate with the
117 device drivers provided by 3D Systems Inc (3D Systems Inc, Rock Hill SC) for their Touch
118 haptic device. The Update function then visually renders the scene and provides the Oculus Rift
119 (Oculus VR, Menlo Park CA) headset with the result.



120

121 **Figure 2.** Simulator software design. Square boxes represent an internal component and rounded boxes represent
 122 output. The Oculus DK 2 and 3D Systems Touch boxes correspond to the VR headset and haptic devices,
 123 respectively (including their drivers and applications).

124

125 **2.3 Hardware**

126 The simulator was developed and tested primarily on an Asus ROG laptop with an Intel i7 quad-
127 core processor and an NVIDIA GTX 960M GPU running Windows 10 as an operating system.
128 The Oculus Rift DK2 was used to allow for an immersive user experience. The use of a VR
129 environment has the additional benefit of providing a sense of depth, which not only improves
130 the user experience of the simulator but also lends it additional realism. When a VR display was
131 not present, the simulator was rendered on the laptop screen, which was a 15-inch, 1080p
132 display. Unity3D provides extensive support for Oculus VR development. To allow for VR and
133 non-VR use of the simulator, scenes included an additional camera exclusively for VR use. A
134 monitor script checked for the presence of a VR device at run-time and adjusted the simulator
135 accordingly.

136 Haptic support was enabled by the 3D Systems Touch device. This device provides six positional
137 degrees of freedom (DOF) and three DOFs for haptic feedback. The Touch device was used to
138 control the position and movement of the electrode and provide the tactile response upon contact
139 with the cochlear anatomy. Unity3D does not natively provide haptic device integration, so C#
140 wrapper functions were created to interface with the 3D System Inc plugins.

141

142 **2.4 Cochlear Models**

143 High resolution (9 μm voxel size) images of multiple cochleae were collected from a previously
144 published study using synchrotron-radiation phase-contrast imaging (SR-PCI) (Elfarnawany et
145 al., 2017). Using 3D Slicer (Fedorov et al., 2012) and Geomagic Studio (3D Systems Inc, Rock
146 Hill SC) a 3D model of the cochlea showing clinically-important internal structures was
147 developed. The open-source software Blender (Blender Foundation, Amsterdam Netherlands)

148 was then used to create an external (outward-facing) surface. This was required since Unity3D
149 only supports single-sided geometry. Therefore, a duplicated surface of the cochlea was created
150 and fitted to the existing surface. The new surface then had its normal vectors flipped. Both the
151 single-sided and double-sided models were imported into Unity3D. Using the Unity3D editor,
152 mesh colliders were applied. The use of single-sided and double-sided mesh geometry allows the
153 user to select whether the simulated cochlea's external faces are transparent. The mesh colliders
154 were required for the detection of collision events with the electrode during the simulation.
155 Anatomical features, such as the basilar membrane (an intracochlear membrane which should be
156 kept intact during insertion), were segmented from the SR-PCI data independently, and
157 developed into their own 3D models before being combined in Unity3D. By doing this, the
158 different physical and haptic features could be applied to different anatomical structures in an
159 efficient manner.

160

161 **2.5 Electrode Modelling**

162 Since Unity3D does not natively support bendable objects, a custom implementation is needed to
163 simulate many medical procedures. The primary concerns of the electrode simulations were
164 physical realism and efficiency. By modelling the physics of the electrode in real-time, trainees
165 can visualize the electrode coiling into the cochlea, which is not possible during actual surgery
166 due to the opaque bone.

167 To achieve these goals, the electrode was simulated using a mass-spring model. Mass-spring
168 models have long been known to realistically simulate deformable objects and offer several
169 computational advantages in the Unity3D framework (Basdogan, Ho, & Srinivasan, 2001;

170 Luboz, Blazewski, Gould, & Bello, 2009). The “masses” of the electrode object were represented
171 by capsules (a Unity3D primitive object). This greatly reduced the number of draw calls required
172 to render the electrode, since Unity3D supports GPU instancing to draw multiple copies of the
173 same mesh (Unity3D, 2018). Each capsule was connected by a Unity3D spring-joint. Spring-
174 joints have customizable physical properties, such as a spring constant and coefficient of
175 damping. These properties were qualitatively tuned to best resemble an electrode by consulting a
176 practicing ear surgeon with over a decade of experience in cochlear implant surgery.

177 In addition to the capsule and spring-joint system, the individual cells of the electrode had scripts
178 and components attached. Each segment of the electrode had an associated rigid-body and a
179 trigger collider. The rigid-body ensured the segment was governed by the physics engine, and the
180 trigger collider provided the ability to raise collision events when specific areas of the electrode
181 entered defined regions of the cochlea.

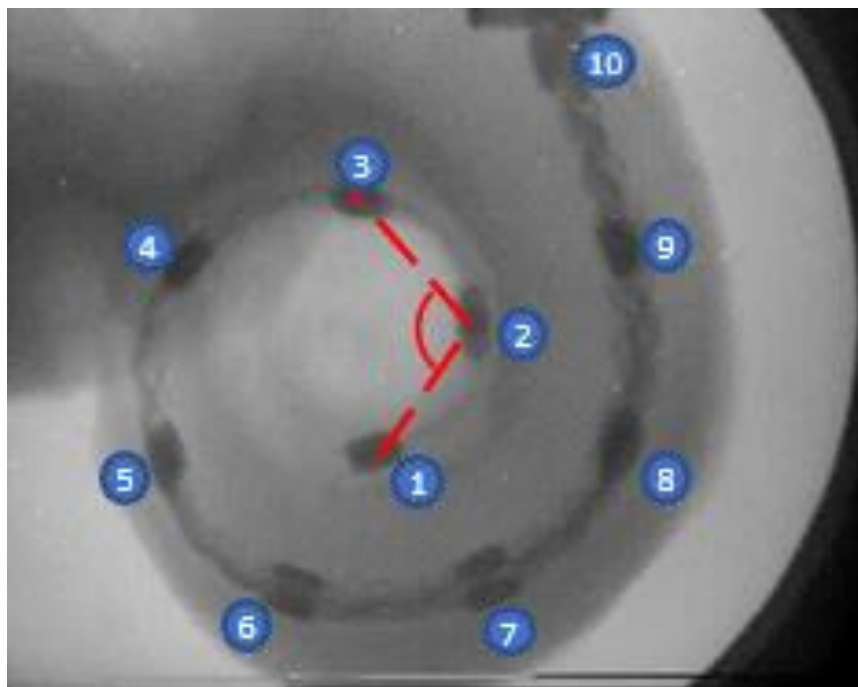
182 **2.6 Assessment of the Simulated Electrode Model**

183 The behaviour of a cochlear implant electrode during insertion has important ramifications for
184 the overall success of the procedure. Limited imaging of an electrode during insertion exists due
185 to the difficulty involved in acquiring such data. To validate the simulated electrode, images
186 from a fluoroscopic video of an actual insertion into a human cochlea were obtained, courtesy of
187 Med-El GmbH (Innsbruck, Austria).

188 A visual comparison with the fluoroscopy data was encouraging, however a quantitative
189 assessment of the behaviour of the simulated electrode was desired. To accomplish this, a novel
190 approach to compare the shape of the electrodes was developed. The method simultaneously

191 considered three consecutive, inserted segments of the electrode and obtained an angle
192 representing the local deformation of the electrode at a particular point.

193 As shown in Figure 3, the first angle was calculated by connecting the centroids of segments 1
194 and 2, and 2 and 3, respectively. The angle between these lines was then recorded. This process
195 then continued using segment 2 as the initial electrode. The final angle was calculated between
196 the lines formed by the centroids of segments 5 and 6, and 6 and 7, respectively. Therefore,
197 every time an additional segment of the electrode entered the cochlea, this set of measurements
198 could be repeated with the newly inserted segment allowing for an additional angle to be
199 calculated. As a result, this method allowed for an evaluation of the electrode bending not only in
200 its final configuration, but at several stages throughout the procedure.



201
202 **Figure 3.** A fluoroscopically-obtained image of an electrode inserted into a human cochlea with the electrode
203 segments numbered (segment 1 being the deepest).

204 Using this method, angles were measured for both the fluoroscopic data and simulation data. The
205 results from multiple simulations were collected and averaged. Both sets of measurements were
206 found to be normally distributed using the Shapiro-Wilk (Shapiro & Wilk, 1965) and Anderson-
207 Darling tests (Stephens, 1974). Therefore, a paired *t*-test was used to evaluate the significant
208 difference between the fluoroscopic and simulated measurements. Significance was set to $p <$
209 0.05. Apart from significance testing, the percent error from each measurement was assessed via
210 the formula presented in Equation 1, where *S* is the value obtained from the simulated electrode
211 and *F* is the value from the fluoroscopic data.

212 Equation 1:
$$Percent\ Error = \frac{S-F}{F} \times 100\%$$

213

214 **3. Results and Discussion**

215 **3.1 Simulator Performance**

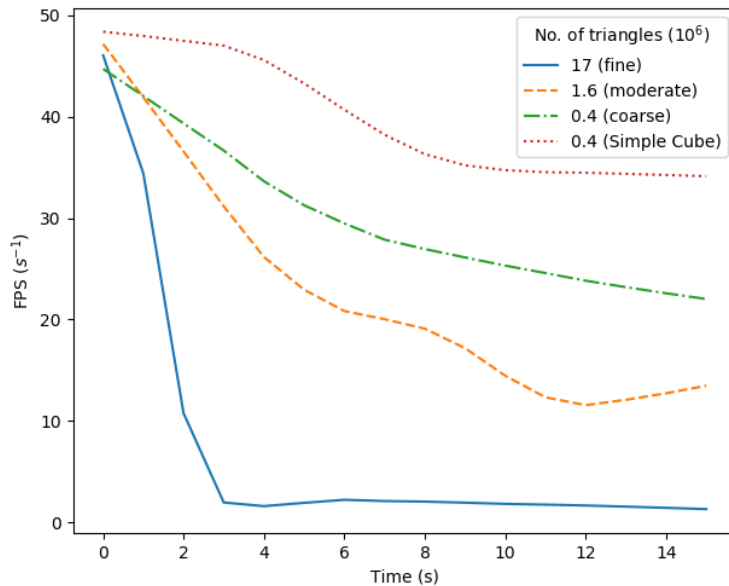
216 The primary goal of this study was to design a simulator to realistically model the behaviour of
217 an electrode during cochlear-implant surgery. It is anticipated that this will improve the
218 understanding of how manipulations performed to the electrode affect the position of the implant
219 during insertion in real-time. As such, the real-time performance of the simulator was of
220 paramount concern. Despite large strides forward in terms of performance, Unity3D has been
221 known to struggle with complex mesh rendering (Cristina, Dapoto, Thomas, & Pesado, 2018).
222 To assess the effectiveness of the simulator, a study of the frame rate as a function of the number
223 of triangles rendered was conducted. Triangles are considered an important aspect of
224 computational load as they form the base unit of graphic rendering. Furthermore, the number of

225 triangles directly correlates with not only the visual fidelity of the model, but also the physical
226 accuracy.

227 Figure 4 shows the recorded frame rate for three cochlear models with a varying number of
228 triangles. Also included in the figure are the frame rate results for a simple cube mesh. To reduce
229 the dependence of the frame rate on specific actions or events, a script was used to move the
230 electrode forward into each of the models at a constant speed. Repeated measurements were
231 taken and then averaged.

232 The frame rate results assisted in choosing an appropriate balance between visual fidelity of the
233 cochlear models and simulator performance. The angle of insertion of the electrode into the
234 cochlea and the speed at which it was inserted were chosen to maximize the number of collisions
235 that the electrode would undergo. Therefore, all the models start at a very similar FPS but are
236 quickly stratified according to mesh detail. The simple cube mesh illustrates the known ability of
237 Unity3D to handle simple meshes and Unity3D primitives with greater efficiency than more
238 complex meshes with a similar level of detail (Cristina et al., 2018).

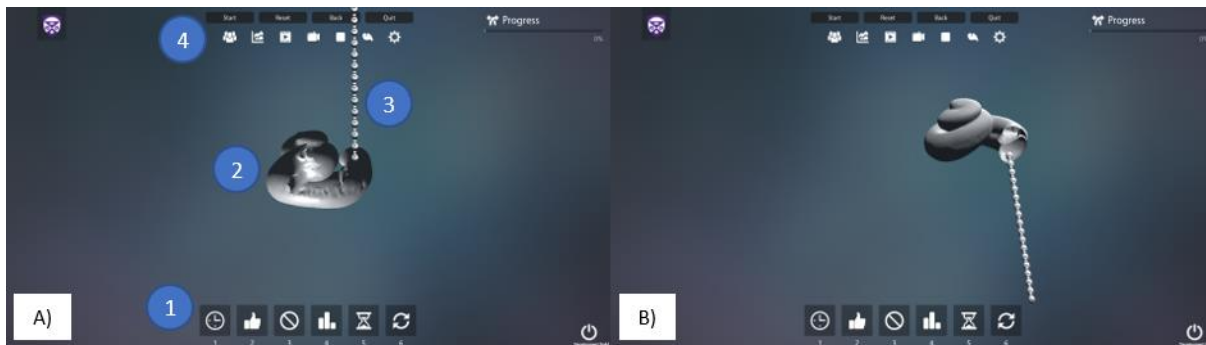
239 A threshold of 20 FPS was deemed as an acceptable minimum to ensure the real-time
240 functionality of the simulator. The smallest model provided a frame rate that was consistently
241 above 20 FPS, even when Unity3D was experiencing an unrealistically high number of
242 collisions. The 359,400 triangles that composed this model offered more than enough detail to
243 accurately render intricate anatomical structures of the SR-PCI models. Figure 5 presents two
244 screenshots from the simulator using cochlear models with a similar level of fidelity as the
245 359,000 triangle benchmark.



246

247 **Figure 4.** The FPS as a function of time for varying levels of mesh triangles and complexity. FPS is the frames per
 248 second of the simulator. Time is correlated to the number of collisions the simulator was modelling, kept consistent
 249 by the controller script (see text for description). As time progressed, the simulator was forced to handle an
 250 increasingly large number of active triangles and collisions, hence the declining FPS with time. The simple cube line
 251 indicates FPS using a simple cube mesh while all other lines result from cochlear meshes. Locally weighed scatter
 252 plot smoothing (LOWESS) with a factor of 0.45 was used.

253



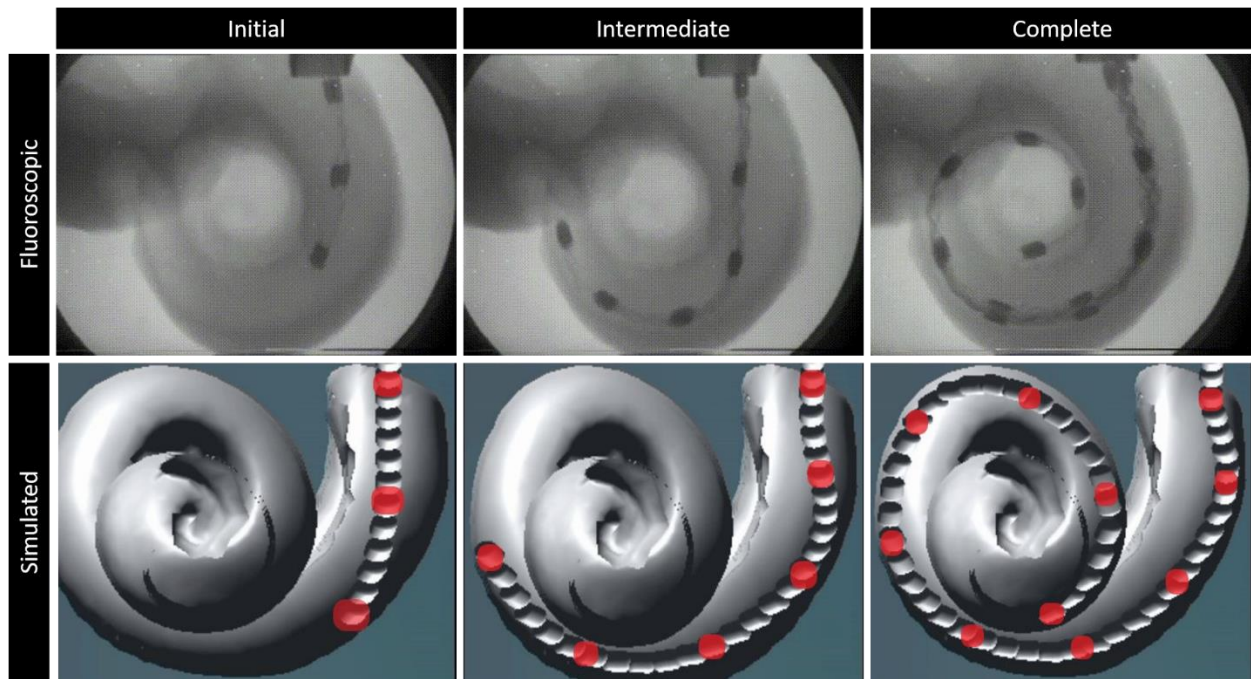
254

255 **Figure 5.** Screenshots of the training scene of the simulator. A) electrode and simple cochlea. The cochlea has its
 256 external faces made transparent allowing for observation of both the internal anatomy and the electrode during
 257 insertion. 1: Basic usage statistic display (insertion time, number of successful insertions, failed attempts, average
 258 insertion depth, total time spent training and number of resets), 2: Cochlear model, 3: The electrode, 4: UI options to
 259 modify simulator settings, begin/end a recording, select a different cochlea model, etc. B) The electrode with a more
 260 complex cochlear model that includes additional anatomical features. The external faces of the model have been
 261 rendered and thus the outward faces of the model are no longer transparent.

262

263 3.2 Simulated Electrode Model

264 The modelled electrode was an important component of the simulator. Our electrode model had a
265 mean angular deformation of 127° and standard deviation of 19.4° , whereas the mean angular
266 deformation of an actual electrode was 129° with a standard deviation of 17.5° . A paired t-test
267 did not reveal a significant difference between the simulated and actual deformations at a p-value
268 of 0.05 ($t=-0.14$, $p=0.89$, $DOF=8$). Figure 6 highlights the qualitative performance of the
269 simulated electrode model. From the comparison of the simulated electrode to the fluoroscopic
270 images, the behaviour of both is consistent throughout the procedure.

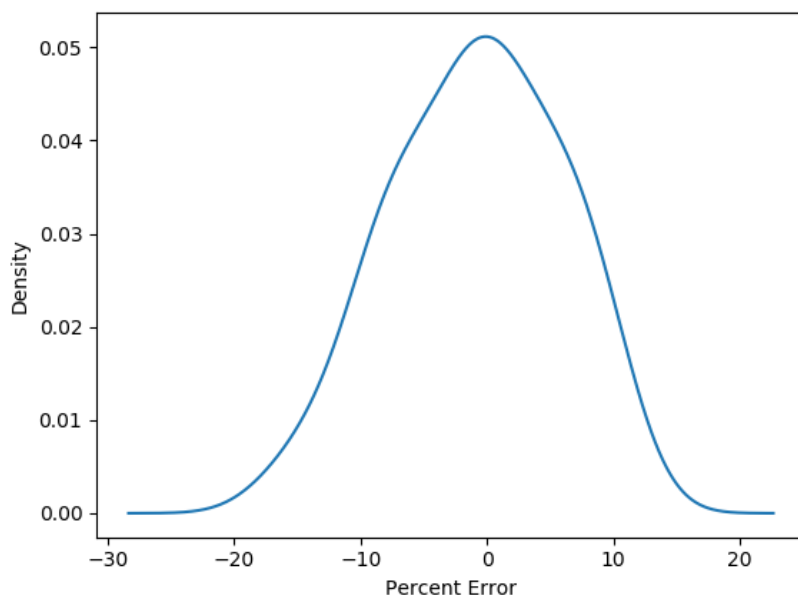


271

272 **Figure 6.** Video frames from a fluoroscopic insertion of an electrode compared to screenshots of an insertion of the
273 simulated electrode at various insertion depths. The red circles indicate the position of the individual electrodes to
274 facilitate easy visual comparison.

275

276 The kernel density estimation of the percent error for all measurements, calculated from
277 Equation 1, is shown in Figure 7. The maximum deviation that occurred between the averaged
278 measurements was 7.2% and the average deviation was <1%.



279

280 **Figure 7.** A Kernel Density Estimation plot of the percent difference between the fluoroscopic and raw simulation
281 data with a mean and standard deviation of 0.83% and 6.57% respectively.

282

283 **3.3 Debriefing Functionality**

284 An extremely useful, but often underutilized, benefit of virtual surgical simulators is their ability
285 to autonomously collect data as students are being trained. The simulator presented here tracks
286 basic usage statistics, and provides instance-specific data on each electrode insertion attempt.
287 Two categories of instance-specific data were collected: 1) force as a function of depth, and 2)
288 depth as a function of time. These statistics are useful for allowing users to debrief after using the
289 simulator and also serve as the basis for automatic error detection and future discriminant

290 validity studies. This data can be examined in application or exported as a JavaScript Object
291 Notation (JSON) file. In addition to numerical feedback, the system allows for users to record
292 their attempts as a video for self or expert review.

293 **3.4 Advantages and disadvantages of Unity3D**

294 A major contribution of this paper was providing a benchmarked example of a surgical simulator
295 that adopted popular gaming technologies. In 2007, Marks *et al* conducted one of the earliest
296 examinations of the potential of game engines in relation to serious game development (Marks,
297 Windsor & Wünsche, 2007). They concluded that the physical realism and technological
298 abstraction that game engines provided was well suited for serious game or simulation
299 development but that the performance was not yet at an acceptable level. More recently, the
300 latency between Unity3D developed applications and VR headsets was probed and found to be
301 comparable to low-level frameworks (Le Chénéchal & Chatel-Goldman, 2018). By providing
302 quantitative outcomes of this system's performance we aimed to update the literature regarding
303 the feasibility of medical simulation on a widely available game engine platform.

304 Unity3D was chosen for the development of the simulator due to its increasingly large presence
305 in professional game development and for its reputation as being a user-friendly framework
306 (Craighead, Burke, & Murphy, 2008). The powerful GUI, highly familiar workflow and wide
307 developer base of Unity3D make it well positioned to reduce the technical cost of simulator
308 development compared to other existing frameworks, like SOFA, discussed below.

309 Since version 5.0, the personal license of Unity3D supports automatic occlusion culling
310 (Unity3D, 2015). Occlusion culling allows for the omission of objects that are not currently
311 visible from the rendering loop. Depending on the particulars of the scene, this can provide a

312 significant reduction in the rendering cost of a scene which often translates to a marked
313 improvement in overall efficiency. Messaoudi *et al* found that the rendering pipeline was, in
314 some instances, responsible for 92% of the CPU load. Another tool that can have profound
315 implications to graphical processing costs is GPU instancing. The use of GPU instancing for this
316 simulator meant that all the segments of the electrode could be drawn in one batch call, thereby
317 preventing a large amount of overhead to draw copies of the same mesh.

318 Apart from graphical rendering, simulations often have an emphasis on realism, which requires
319 accurate physical calculations. The fixed time step in Unity3D controls the time step between
320 physical calculations. A smaller time step can result in more accurate calculations but can
321 significantly impair system performance. Previously, our group has reported the impact of the
322 fixed time step on Unity3D's frame rate (Huang, Agrawal, & Ladak, 2016). A fixed time step of
323 0.002 seconds was selected as an acceptable trade-off between accuracy and framerate.

324 An interesting area of Unity3D that was not utilized in this work is the third-party, performant
325 frameworks that are beginning to interface with Unity3D through the use of application
326 programming interfaces (APIs). Simulation Open Framework Architecture (SOFA) (Allard et al.,
327 2008), a framework written in C++, has specialized in realistic surgical simulation software, runs
328 smoothly in real-time, and is currently in the process of releasing a Unity3D integration.

329 Currently, integration of Unity3D and SOFA is being led by InfinyTech3D (Nice, France) and
330 the first proof-of-concept of SOFA-controlled deformable meshes has recently been released.

331 Although not yet entirely mature, the ability to use third-party libraries like SOFA bodes well for
332 Unity3D's continued role as a platform to develop serious games and simulators.

333 **3.5 Future Work**

334 Using the functional system put forth herein, future work will continue along two main paths in
335 tandem: 1) validity and skill transference studies and 2) the development of standalone mass-
336 spring framework that will be released as an asset on the Unity asset store for public use. Similar
337 to work conducted previously in the lab for an audiological probe tube simulator (Koch *et al*,
338 2018), face and content validity will be assessed with feedback from additional otolaryngologists
339 and medical students. After incorporating the feedback into the simulator, skills transference can
340 proceed and the efficacy of the simulator can be quantitatively assessed.

341 **4. Conclusion**

342 The current work presented a fully implemented virtual-reality simulator of an electrode
343 insertion into human cochleae. The simulator allowed users to repeatedly practice electrode
344 insertions in a safe, controlled environment, with costs that did not increase with usage. The
345 simulator further allowed for the real-time visualization of electrode behaviour during insertion
346 and provided detailed performance metrics as well as the ability to replay video of previous
347 attempts. Continued use of widely available and supported game engines in medical simulation
348 will hopefully result in lowered costs of VR simulators. Preliminary feedback of the simulator
349 from relevant professionals has been positive and future work will focus on evaluating its face,
350 content and construct validity.

351 **Funding Statement**

352 Funding for this work was provided through a Collaborative Health Research Projects grant from
353 the Canadian Institutes of Health Research and from the Natural Sciences and Engineering
354 Research Council of Canada.

355

356 **References**

- 357 Allard, J., Cotin, S., Faure, F., Bensoussan, P., Poyer, F., Duriez, C., Delingette, H., & Grisoni,
358 L. (2007). SOFA - an Open Source Framework for Medical Simulation. *Studies in health*
359 *technology and informatics*, 125, 13-8.
- 360 Basdogan, C., Ho, C. H., & Srinivasan, M. A. (2001). Virtual environments for medical training:
361 Graphical and haptic simulation of laparoscopic common bile duct exploration. *IEEE/ASME*
362 *Transactions on Mechatronics*, 6(3), 269–285. <https://doi.org/10.1109/3516.951365>
- 363 Coles, T. R., Meglan, D., & John, N. W. (2011). The role of haptics in medical training
364 simulators: A survey of the state of the art. *IEEE Transactions on Haptics*, 4(1), 51–66.
365 <https://doi.org/10.1109/TOH.2010.19>
- 366 Connell, B. P. O., Hunter, J. B., & Wanna, G. B. (2016). The Importance of Electrode Location
367 in Cochlear Implantation, (December), 169–174. <https://doi.org/10.1002/lio2.42>
- 368 Jeff Craighead, Jenny Burke, Robin Murphy. “Using the Unity Game Engine to Develop
369 SARGE: A Case Study”. Proceedings of the 2008 Simulation Workshop at the International
370 Conference on Intelligent Robots and Systems (IROS 2008). September 2008.
- 371 Cristina F., Dapoto S., Thomas P., Pesado P. (2018) Performance Evaluation of a 3D Engine for
372 Mobile Devices. In: De Giusti A. (eds) Computer Science – CACIC 2017. CACIC 2017.
373 Communications in Computer and Information Science, vol 790. Springer, Cham.
374 https://doi.org/10.1007/978-3-319-75214-3_15
- 375 Elfarnawany, M., Alam, S. R., Rohani, S. A., Zhu, N., Agrawal, S. K., & Ladak, H. M. (2017).
376 Micro-CT versus synchrotron radiation phase contrast imaging of human cochlea. *Journal*

377 of *Microscopy*, 265(3), 349–357. <https://doi.org/10.1111/jmi.12507>

378 Escobar-Castillejos, D., Noguez, J., Neri, L., Magana, A., & Benes, B. (2016). A Review of
379 Simulators with Haptic Devices for Medical Training. *Journal of Medical Systems*, 40(4),
380 1–22. <https://doi.org/10.1007/s10916-016-0459-8>

381 Fedorov, A., Beichel, R., Kalphaty-Cramer, J., Finet, J., Fillion-Robbin, J.-C., Pujol, S., ...
382 Kikinis, R. (2012). 3D Slicer as an image computing platform for the quantitative imaging
383 network. *Magnetic Resonance Imaging*, 30(9), 1323–1341.
384 <https://doi.org/10.1016/j.mri.2012.05.001>

385 Finley, C. C., Holden T.A., Holden L. K., Whiting B. R., Chole R. A., Neely G. J., Hullar T. E.,
386 Skinner, M. W. (2009). Role of electrode placement as a contributor to variability in
387 cochlear implant outcomes. *Otology and Neurotology*, 29(7), 920–928.
388 <https://doi.org/10.1097/MAO.0b013e318184f492>

389 Grand View Research. (2017). *Cochlear Implants Market Analysis By Type of Fitting (Unilateral*
390 *Implantation, Bilateral Implantation), By End-Users (Adults, Pediatrics), By Region (North*
391 *America, Europe, APAC, Latin America, MEA), & Segment Forecasts, 2018 - 2025.*
392 Retrieved from [https://www.grandviewresearch.com/industry-analysis/cochlear-implants-](https://www.grandviewresearch.com/industry-analysis/cochlear-implants-industry)
393 industry

394 Huang, C., Agrawal, S. K., & Ladak, H. M. (2016). Virtual Reality Simulator for Training in
395 Myringotomy with Tube Placement. *Journal of Medical and Biological Engineering*, 36(2),
396 214–225. <https://doi.org/10.1007/s40846-016-0124-1>

397 Koch RW, Moodie S, Folkeard P, Scollie S, Janeteas C, Agrawal SK, Ladak HM. (2018). Face

398 and Content Validity of a Probe Tube Placement Training Simulator. *J Am Acad Audiol*.
399 DOI:10.3766/jaaa.17114. PMID: 30461412.

400 Kotsis, S. V., & Chung, K. C. (2013). Application of the “see one, do one, teach one” concept in
401 surgical training. *Plastic and Reconstructive Surgery*, *131*(5), 1194–1201.
402 <https://doi.org/10.1097/PRS.0b013e318287a0b3>

403 Le Chénéchal, M., Chatel-Goldman, J. (2018) HTC Vive Pro time performance benchmark for
404 scientific research. ICAT-EGVE 2018, Limassol, Cyprus.

405 Luboz, V., Blazewski, R., Gould, D., & Bello, F. (2009). Real-time guidewire simulation in
406 complex vascular models. *Visual Computer*, *25*(9), 827–834.
407 <https://doi.org/10.1007/s00371-009-0312-x>

408 Marks, S., Windsor, J., & Wünsche, B. 2007. Evaluation of game engines for simulated surgical
409 training. In Proceedings of the 5th international conference on Computer graphics and
410 interactive techniques in Australia and Southeast Asia (GRAPHITE '07). ACM, New York,
411 NY, USA, 273-280. DOI: <https://doi.org/10.1145/1321261.1321311>

412 F. Messaoudi, G. Simon and A. Ksentini, "Dissecting games engines: The case of Unity3D,"
413 2015 International Workshop on Network and Systems Support for Games (NetGames),
414 Zagreb, 2015, pp. 1-6. DOI: 10.1109/NetGames.2015.7382990

415 Nagendran M, Gurusamy KS, Aggarwal R, Loizidou M, Davidson BR. Virtual reality training
416 for surgical trainees in laparoscopic surgery. *Cochrane Database of Systematic Reviews*
417 2013, Issue 8. Art. No.: CD006575. <https://doi.org/10.1002/14651858.CD006575.pub3>.

418 NIDCD. (2017). Cochlear Implants. Retrieved May 28, 2018, from the National Institute on

419 Deafness and Other Communication Disorders: <https://www.nidcd.nih.gov/health/cochlear->
420 implants

421 Prasad, M. S. R., Manivannan, M., Manoharan, G., & Chandramohan, S. M. (2016). Objective
422 Assessment of Laparoscopic Force and Psychomotor Skills in a Novel Virtual Reality-
423 Based Haptic Simulator. *Journal of Surgical Education*, 73(5), 858–869.
424 <https://doi.org/10.1016/j.jsurg.2016.04.009>

425 Secin, F. P., Savage, C., Abbou, C., de La Taille, A., Salomon, L., Rassweiler, J., Hruza, M.,
426 Rozet, F., Cathelineau, X., Janetschek, G., Nassar, F., Turk, I., Vanni, A. J., Gill, I. S.,
427 Koenig, P., Kaouk, J. H., Martinez Pineiro, L., Pansadoro, V., Emiliozzi, P., Bjartell, A.,
428 Jiborn, T., Eden, C., Richards, A. J., Van Velthoven, R., Stolzenburg, J. U., Rabenalt, R.,
429 Su, L. M., Pavlovich, C. P., Levinson, A. W., Touijer, K. A., Vickers, A., ... Guillonau,
430 B. (2010). The learning curve for laparoscopic radical prostatectomy: an international
431 multicenter study. *The Journal of urology*, 184(6), 2291-6.

432 Shapiro, S. S. and Wilk, M. B. (1965). An analysis of variance test for normality (complete
433 samples). *Biometrika*, 591–611.

434 Stephens, M. A. (1974). EDF Statistics for Goodness of Fit and Some Comparisons. *Journal of*
435 *the American Statistical Association*, 69, 730–737.

436 Unity3D. (2015). Unity 5.0 Release Notes. Retrieved May 28, 2018, from
437 <https://unity3d.com/unity/whats-new/unity-5.0>

438 Unity3D. (2018). Unity - Manual: GPU instancing. [online] Available at:
439 <https://docs.unity3d.com/Manual/GPUInstancing.html>

440 Wikimedia Commons. (2008). Cochlea Implant. Retrieved May 29, 2018, from

441 <https://commons.wikimedia.org/wiki/File:Cochleaimplantat.jpg>

442